Optimal Heterogeneity for Coding in Spiking Neural Networks

J. F. Mejias[1,*] and A. Longtin[1]

[1]*Department of Physics and Center for Neural Dynamics, University of Ottawa, 150 Louis Pasteur, K1N-6N5 Ottawa, ON, Canada*

(Dated: April 14, 2012)

The effect of cellular heterogeneity on the coding properties of neural populations is studied analytically and numerically. We found that heterogeneity decreases the threshold for synchronization, and its strength is nonlinearly related to network mean firing rate. In addition, conditions are shown under which heterogeneity optimizes network information transmission for either temporal or rate coding, with high input frequencies leading to different effects for each coding strategy. The results are shown to be robust for more realistic conditions.

Neural ensembles detect and process information embedded in external signals by employing a wide set of strategies. Typical examples include the frequency-dependent gain control associated with activity-dependent synapses [1, 2], detection of coincident spikes aided by neural or synaptic adaptation [3, 4], or stochastic resonance mechanisms [5, 6]. When addressing these and other mechanisms of information processing, the vast majority of studies assume for simplicity networks of identical neurons.

Actual neural systems, however, display a prominent heterogeneity in neuron properties, even among same-class neurons, and this may have strong implications for information processing. A well-known example is the so called *population coding*, a strategy which relies on the particular responses of individual neurons of a network to code information. This occurs for instance in V1 cortical networks, where the orientation preference of neurons allows for efficient information coding [7, 8]. However, very few attempts have been made to understand the role of neural heterogeneity in other neural coding strategies. Recently, cell-to-cell differences have been found to be relevant in many contexts, such as in synchronization of inhibitory networks [9, 10] or excitatory ones [11, 12], coherent activity in electrically coupled neurons [13], synchronized bursting events [14], global detection of weak signals [15, 16], or envelope and temporal processing [17]. Attending to these findings, it is plausible that neural heterogeneity may greatly influence the performance of neural populations when detecting and processing external stimuli. Neither the effect of heterogeneity on the dynamics of neural populations nor its influence on neural coding are yet fully understood.

In this Letter, we present a theoretical and numerical study of the implications of heterogeneity for the properties of neural populations, and in particular for their ability to detect and codify incoming signals. We start by showing the precise effects that neural heterogeneity has on the mean firing rate and the synchronization properties of the network. Then, we find that these effects have strong consequences for two main information processing strategies used in many brain areas: rate coding and temporal coding. More concretely, we show that certain heterogeneity values–which lie within the physiological rage found in actual neurons– optimize the transmission of information in rate and temporal codes, suggesting that cell-to-cell differences are not useful only for population coding, but also for more general coding strategies.

We assume a fully connected network of N excitatory integrate-and-fire neurons, each one governed by the dynamics

$$\tau_m \frac{dV_i(t)}{dt} = -V_i(t) + RI_i^{ext}(t) + RI_i^{net}(t), \qquad (1)$$

where τ_m is the neuron membrane time constant, V_i is the membrane potential of the $i-th$ neuron in the network, R is the membrane resistance, and I_i^{ext}, I_i^{net} are the external and recurrent input to the $i-th$ neuron, respectively. Each neuron i is assumed to fire an action potential (AP) every time V_i reaches a certain firing threshold, and after that the membrane potential is reset to V_r for a time period τ_{ref}. The external and recurrent input to the $i-th$ neuron are given, respectively, by

$$I_i^{ext}(t) = \mu + \sigma\sqrt{\tau_m}\xi_i(t), \qquad (2)$$

$$I_i^{net}(t) = \frac{\tau_m}{N}\sum_j \sum_k J\ \delta(t - t_{ij}^k - D), \qquad (3)$$

where μ is a constant input bias, $\xi_i(t)$ is a gaussian white noise of zero mean and unitary variance, σ is the noise intensity, J is the synaptic coupling strength, and the $k-th$ spike from neuron j arrives at neuron i at $t_{ij}^k + D$, with D being a small synaptic delay.

In this framework, each neuron is characterized by a different distance-to-threshold value, which may be related to different neuronal features (such as reset potential, firing threshold, leak or other conductances etc...). We assume here that such heterogeneity in the distance-to-threshold corresponds to heterogeneity in firing threshold values. Therefore, each neuron has a firing threshold θ_i which is randomly distributed following a gaussian profile $P(\theta)$ with mean $\overline{\theta}$ and standard deviation w. Such heterogeneity reflects some of the variability in the individual excitability properties of neurons found in actual neural systems.

We may obtain the stationary firing rate of the model by employing a mean-field description based on the one presented in [18, 19]. Considering the diffusion approximation, the recurrent part of the current can be written as $I^{net} = \tau_m J\ \nu_0$, where ν_0 is the stationary mean firing rate of the network, assuming asynchronous network states [19]. Eq. (1) appears then as a Langevin equation of the form $\tau_m \dot{V}_i = -V_i + \mu_d + \sigma\sqrt{\tau_m}\xi_i(t)$, where $\mu_d = \mu + \tau_m J\ \nu_0$ is the deterministic part of the current. The mean firing rate of the i-th neuron in stationary conditions [18] is then $\nu_i = \left[\tau_{ref} + \tau_m \int_{y_r}^{y_i} f(z)dz\right]^{-1}$, where $y_i = \frac{\theta_i - \mu_d}{\sigma}$, $y_r = \frac{V_r - \mu_d}{\sigma}$ and $f(z) = \sqrt{\pi}\exp(z^2)(1 + \mathrm{erf}(z))$. In order to obtain the stationary mean firing rate of the network, we must average over all the stationary neuron rates. For large enough networks ($N \to \infty$), it is a good approximation to substitute the sum over neuron firing rates by an integral over the network firing rates, given a probability distribution of rates $\mathcal{P}(\nu)$, that is,

$$\nu_0 = \frac{1}{N}\sum_{i=1}^{N} \nu_i \simeq \int_0^{1/\tau_{ref}} \nu\ \mathcal{P}(\nu)d\nu \qquad (4)$$

Assuming that the variability in neuron firing rates is mainly due to the heterogeneity of firing thresholds, one can arrive to the following equation for ν_0:

$$\nu_0 = \int_{\theta_{min}}^{\theta_{max}} \left[\tau_{ref} + \tau_m \int_{y_r}^{y_\theta} f(z)dz\right]^{-1} P(\theta)d\theta, \qquad (5)$$

where $y_\theta = \frac{\theta - \mu_d}{\sigma}$, and θ_{min}, θ_{max} are the integration intervals. These intervals, in practice, must satisfy $\theta_{max} \gg \overline{\theta} + w$, and $V_r \ll \theta_{min} \ll \overline{\theta} - w$. Such restrictions impose a range of validity of w for our theory, however, this range is wide enough to include the values observed in experiments, with w being around a few millivolts [20]. Note that, due to the presence of ν_0 in μ_d, Eq. (5) must be numerically solved to obtain ν_0. In the following, we rename the right-hand side of Eq. (5) as $\Phi(\nu_0, w)$.

The effect of heterogeneity on the mean firing rate of the network can be seen in Fig. 1A: the mean firing rate increases with the level of heterogeneity, up to several times its initial ($w = 0$) value for relatively low w. This relationship is approximately quadratic in w for low values of heterogeneity, suggesting that the firing rate depends on the variance of thresholds. Such a dramatic increase with w can be explained if we consider that, for $w > 0$, the existence of a significant number of low-threshold neurons induces an extra current to the neurons with high-threshold, and the overall effect is an increase in the network firing rate. Our theoretical predictions agree very well with the numerical simulations for different values of the input current μ. Low-threshold neurons do not only induce an extra current to the network, but also allow for an easier synchronization due to their high firing rate. This may be analyzed by employing a simplified treatment of the firing rate dynamics of our system.

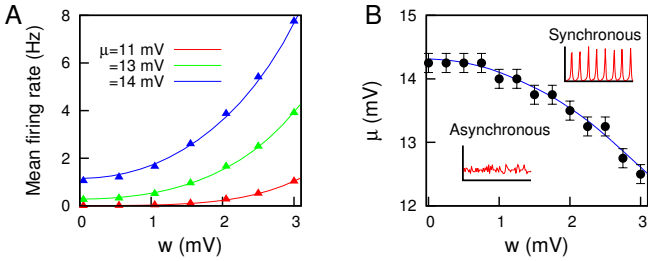

FIG. 1: (A) Network mean firing rate ν_0 as a function of the level of heterogeneity w for 3 bias values. (B) Stability line separating the asynchronous and synchronous regimes. In both panels, numerical simulations of Eqs.(1)-(3) (points) confirm our mean-field predictions (lines). Insets in (B) show a typical time evolution of the mean firing rate for the corresponding behavior. Coupling strength J is 10 mV (A) or 20 mV (B). Here and below, unless specified otherwise, we have $N = 1500$, $\tau_m = 20$ ms, $R = 0.1$ $G\Omega$, $V_r = 10$ mV, $\tau_r = 5$ ms, $D = 2$ ms, $\overline{\theta} = 20$ mV and $\sigma = 3$ mV.

Concretely, for asynchronous activity states, one may assume that the dynamics of the network firing rate evolves according to $\tau_\nu\ \dot{\nu} = -\nu + \Phi(\nu, w)$, where we set $\tau_\nu \simeq 3$ ms as the typical time scale of the rate dynamics [21]. Using standard techniques to study the linear stability of this dynamics, one arrives at the local stability condition

$$\int_{\theta_{min}}^{\theta_{max}} \frac{\tau_m^2 J\ [f(y_\theta) - f(y_r)]\, P(\theta)}{\sigma\left[\tau_{ref} + \tau_m \int_{y_r}^{y_\theta} f(z)dz\right]^2}\, d\theta < 1, \qquad (6)$$

assuming, for simplicity, $D \sim 0$. Figure 1B presents a phase diagram displaying the synchronous and asynchronous regimes of the system, and reveals the existence of a critical stability line separating both regimes. Numerical simulations as well as theoretical predictions indicate that networks of heterogeneous neurons need weaker constant inputs to display collective synchronous activity. It also shows that a homogeneous neural network may enter the synchronous regime by simply increasing its level of heterogeneity (using, for instance, input-driven cellular homeostatic mechanisms [20]). The synchronous regime referred here differs from the one found in networks with inhibitory neurons, which involves fast oscillations without strong cell-to-cell synchronization [19].

Taking into account these findings, one may wonder about the implications that neural heterogeneity could have for information processing tasks, via the two heterogeneity-induced effects described above. The implications of the increment of ν_0 with w may be investigated by considering that, instead of having a constant input μ, each neuron now receives an external input given by $\mu + S(t)$, where $S(t) = A_s \sin(2\pi f_s t)$ stands for a weak, slow modulation ($1/f_s > \tau_\nu$). Such modulation could reflect information encoded in brain waves and transmitted from other brain areas, a mechanism that has been associated with high-level integration of information [22].

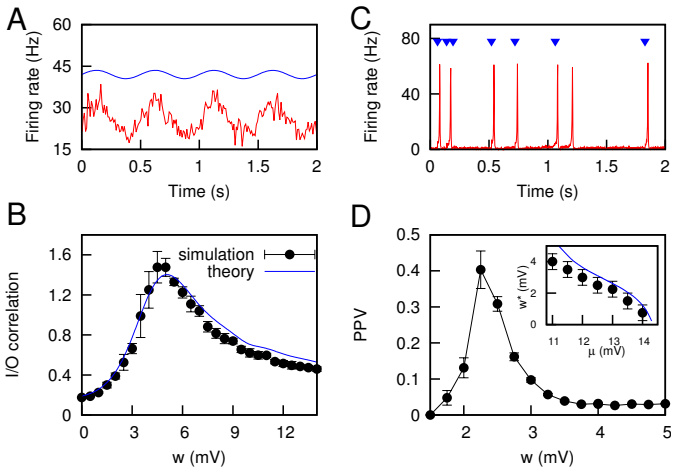

FIG. 2: (A) Time varying firing rate (red) of an heterogeneous ($w = 4\ mV$) neural population to a slowly modulated signal (blue line) in the asynchronous regime, corresponding to a rate coding scheme. (B) Input-output correlation as a function of w. (C) Response of an heterogeneous ($w = 2.5\ mV$) neural population, close to the stability line, to a train of delta-like pulses (blue triangles), corresponding to a temporal coding scheme. (D) PPV is optimized for a given value of the heterogeneity. The time window used to identify a TP event was $\Delta t = 10\ ms$. Inset: as suggested by our analysis, w^* closely follows the mean-field stability line (blue line).For panels A, B: $\mu = 14\ mV$, $J = 10\ mV$, $A_s = 0.5\ mV$ and $f_s = 2\ Hz$. For panels C, D: $\mu = 14\ mV$ (varying in inset), $J = 20\ mV$, $A_p = 1\ mV$, $f_p = 3\ Hz$.

In asynchronous conditions, the network may be able to detect and transmit the slowly-modulated signal by modulating its own mean firing rate to follow the signal (see Fig. 2A), a strategy known as rate coding [23, 24]. Since the relationship $\nu_0 - w$ is nonlinear, one could expect different levels of linear performance on this task depending on the level of heterogeneity. Indeed, as Fig. 2B shows, the coding efficiency of the slowly-modulated signal (measured as a standard input-output correlation between the input signal and the network mean firing rate) is optimized for a given (nonzero) value of neural heterogeneity, in a stochastic resonance-like fashion [15, 16, 25]. Interestingly, the optimal value (which we denote as w^* hereafter) is approximately $w^* \sim 4\ mV$, a value which is close to the firing threshold variability found, for instance, in cortical areas [20]. Thus, a moderate level of cell-to-cell differences may optimize, via rate coding strategies, the transmission of information embedded in brain waves from another cortical regions. The effects of heterogeneity on synchronization may also play an important role in information processing. We studied this possibility by considering that, in addition to a constant input μ, neurons receive coincident delta-like impulses of small amplitude A_p, where the time intervals between impulses follow a Poisson distribution of mean rate f_p. Such stimuli resemble highly synchronized events coming from other brain areas, and constitute a weak signal of pulses precisely localized in time. From Fig. 1B, one could expect that networks with different heterogeneity levels respond differently to weak pulses, because of their different distances to the stability line. In particular (see Fig. 2C), networks which are close to the stability line are expected to display enhanced sensitivity to weak stimuli, producing highly synchronized population spikes as an immediate response to an input pulse[26]. Such a detection strategy, which strongly relies on the generation of sharp responses precisely located in time, is known as temporal coding [23, 24]. In order to measure the time coincidence of input and output events, we employ the positive predictive value (PPV) from receiver operating characteristic (ROC) theory, which is defined as $PPV = TP/(TP + FP)$, with TP, FP being the number of true positive and false positive detections, respectively [27]. As Fig. 2D shows, the efficiency of the system to detect input pulses (measured as the PPV) is bell-shaped, with an optimal value of neural heterogeneity of $w^* \sim 2\ mV$. This dependence indicates the existence of an optimal neural heterogeneity level for the detection of precisely-timed events under temporal coding strategies. As predicted, such optimal heterogeneity level w^* is close to the stability line (inset of Fig. 2D), where sensitivity to small inputs is enhanced.

We can further characterize the role of heterogeneity on rate and temporal coding. For the rate coding scheme, we study the optimal heterogeneity value w^* as a function of the modulation frequency f_s. As Fig. 3A shows, w^* increases with f_s, indicating that networks with low (high) levels of neural heterogeneity are better fitted for processing information embedded in slow (fast) brain waves. The modulation frequency does not have a strong influence on the peak value of the I/O correlation for $f_s \lesssim 30\ Hz$. Figure 3B plots w^* for different brain wave regimes. It also shows that the dependency $w^* - f_s$ follows an exponential function, suggesting that heterogeneity in neuronal properties may serve to nicely discriminate among high-frequency signals, since a network will detect properly a signal of a given frequency f, but not those of frequencies $f + \delta f$.

Attending to the temporal coding strategy, we have also studied the effect that the mean pulse rate, f_p, has on the detection abilities of the network. Fig. 3C shows that larger f_p values tend to increase the peak value of the positive predictive value (namely PPV^*), but not the value of w at which the peak is found, which is maintained at $w^* \sim 2.5\ mV$. Therefore, the phenomenon is robust for different input rates, and efficiency of temporal coding in networks with $w \sim w^*$ will increase with f_p. Such findings, together with results shown in Fig. 3A,B, also indicate that the effects of the characteristic input frequency on information transmission depend on the coding strategy. Fig. 3D shows the dependence of PPV^* with f_p.

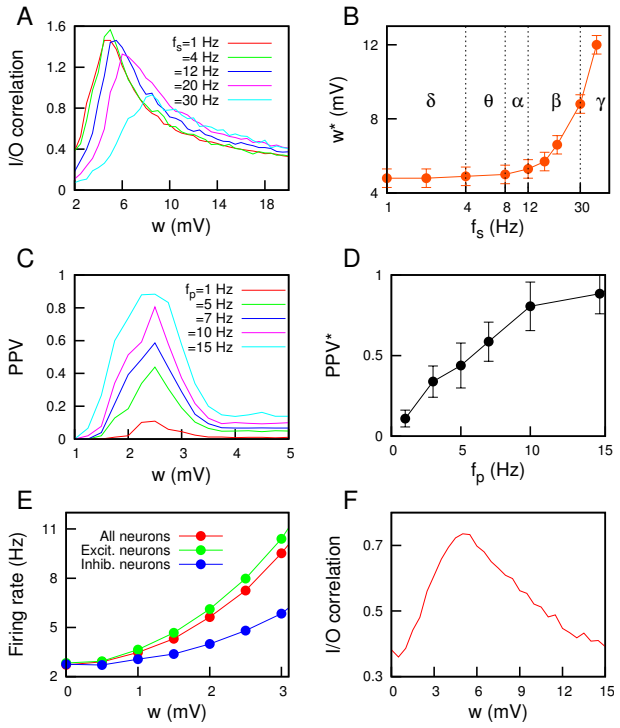

FIG. 3: (A) Input-output correlation as a function of w for different modulation frequencies f_s in the rate coding scheme. (B) Dependence of the optimal heterogeneity level w^* on f_s. Labels indicate the type of brain wave corresponding to this region. For both panels (A and B), $A_s = 0.5\ mV$, $J = 10\ mV$ and $\mu = 14\ mV$. (C) PPV as a function of w for different values of f_p, in the temporal coding scheme. (D) Dependence of the peak value PPV^* on f_p. For both panels (C and D), $A_p = 1\ mV$, $J = 20\ mV$ and $\mu = 13\ mV$. (E) Mean firing rate for a network of 800 excitatory and 200 inhibitory neurons. Connectivity is sparse (400 afferent connections per neuron), coupling strength is 30 mV for excitatory synapses and $-60\ mV$ for inhibitory ones. Panel (F) shows the I/O correlation for such realistic network with an input sine wave as in Fig. 2A, except for $\mu = 15\ mV$.

We have successfully tested our results in more realistic situations, including sparsely connected networks with excitatory and inhibitory populations. As an example, Fig. 3E,F shows the robustness of our findings for the rate coding scheme in such systems, where inhibition simply modifies the I-f curve (this is also true for temporal coding –not shown). Preliminary results reveal the robustness to the inclusion of dynamic synapses.

Summarizing, our theory and numerics show that heterogeneity benefits not only population coding, but also rate and temporal coding strategies. In particular, neural heterogeneity produces a nonlinear increment in the network mean firing rate, and such nonlinear increment leads to an enhancement of signal detection under rate coding. On the other hand, networks of heterogeneous neurons synchronize more easily, which may be used by the system to improve the detection of weak, fast stimuli under temporal coding. Recent experimental findings suggest, indeed, that cell-to-cell differences may play a positive role in processing the information of small and big chirps in the brain of the electric fish for both rate and temporal coding [28], which supports our hypothesis. It is worth noting that the analytical approach that we developed here may be useful for more general studies, since it is valid for subthreshold as well as suprathreshold neural dynamics, for a wide type of inputs, and for weak or strong coupling. Our results also suggest a novel research direction aimed at understanding the role of heterogeneity on other coding strategies such as correlation coding [29, 30].

We acknowledge NSERC Canada for financial support, and Nicolas Brunel for discussions.

* Electronic address: jmejias@uottawa.ca

[1] L. F. Abbott, J. A. Valera, K. Sen, and S. B. Nelson, Science **275**, 220 (1997).
[2] H. Markram, Y. Wang, and M. Tsodyks, Proc. Natl. Acad. Sci. USA **95**, 5323 (1998).
[3] V. Matveev and X. J. Wang, Cerebral Cortex **10**, 1143 (2000).
[4] J. F. Mejias and J. J. Torres, J. Comput. Neurosci. **24**, 222 (2008).
[5] K. Wiesenfeld and F. Moss, Nature **373**, 33 (1995).
[6] J. F. Mejias and J. J. Torres, PLoS One **6**, e17355 (2011).
[7] D. H. Hubel and T. N. Wiesel, J. Physiol. **195**, 215 (1968).
[8] G. H. Henry, B. Dreher, and P. O. Bishop, J. Neurophysiol. **37**, 1394 (1974).
[9] D. Golomb and J. Rinzel, Phys. Rev. E **48**, 4810 (1993).
[10] S. S. Talathi, D. U. Hwang, and W. L. Ditto, J. Comput. Neurosci. **25**, 262 (2008).
[11] L. Neltner, D. Hansel, G. Mato, and C. Meunier, Neural Comput. **12**, 1607 (2000).
[12] D. Golomb, D. Hansel, and G. Mato, in *Handbook of Biological Physics* (2001), vol. 4, pp. 887–968.
[13] S. Ostojic, N. Brunel, and V. Hakim, J. Comput. Neurosci. **26**, 369 (2009).
[14] E. Persi, D. Horn, V. Volman, R. Segev, and E. Ben-Jacob, Neural Comput. **16**, 2577 (2004).
[15] C. J. Tessone, C. R. Mirasso, R. Toral, and J. D. Gunton, Phys. Rev. Lett. **97 (19)**, 194101 (2006).
[16] T. Perez, C. R. Mirasso, R. Toral, and J. D. Gunton, Phil. Trans. R. Soc. A **368**, 5619 (2010).
[17] M. Savard, R. Krahe, and M. J. Chacron, Neurosci. **172**, 270 (2011).
[18] H. C. Tuckwell, *Introduction to theoretical neurobiology. Volume 2: nonlinear and stochastic theories* (Cambridge, 1989).
[19] N. Brunel, J. Comput. Neurosci. **8**, 183 (2000).
[20] R. Azouz and C. M. Gray, Proc. Natl. Acad. Sci. USA **97**, 8110 (2000).
[21] W. Gerstner, Neural Comput. **12**, 43 (2000).
[22] L. L. Colgin, T. Denninger, M. Fyhn, T. Hafting, T. Bonnevie, O. Jensen, M. B. Moser, and E. I. Moser, Nature **462**, 353 (2009).

[23] A. Borst and F. E. Theunissen, Nat. Neurosci. **2**, 947 (1999).
[24] A. Kumar, S. Rotter, and A. Aertsen, Nat. Rev. Neurosci. **11**, 615 (2010).
[25] J. J. Collins, C. C. Chow, and T. T. Imhoff, Phys. Rev. E **52**, 3321 (1995).
[26] G. Fuhrmann, I. Segev, H. Markram, and M. Tsodyks, J. Neurophysiol. **87**, 140 (2001).
[27] X. H. Zhou, N. A. Obuchowski, and D. M. McClish, *Statistical Methods in Diagnostic Medicine* (Wiley and Sons, 2002).
[28] G. Marsat and L. Maler, J. Neurophysiol. **104**, 2543 (2010).
[29] A. L. Jacobs, G. Fridman, R. M. Douglas, N. M. Alam, P. E. Latham, G. T. Prusky, and S. Nirenberg, Proc. Nat. Acad. Sci. USA **106**, 5936 (2009).
[30] W. Nesse, L. Maler, and A. Longtin, Proc. Nat. Acad. Sci. USA **107**, 21973 (2010).